DOI:10.1021/jf9020152

JOURNAL OF AGRICULTURAL AND FOOD CHEMISTRY
ARTICLE

Phytochelatin Synthase Is Regulated by Protein Phosphorylation at a Threonine Residue Near Its Catalytic Site

Hsin-Chieh Wang,[†,‖] Jiann-Shing Wu,[§,‖] Ju-Chen Chia,[†] Chien-Chih Yang,[†] Yu-Jen Wu,[#] and Rong-Huay Juang*,[†]

[†]Department of Biochemical Science and Technology and Institute of Microbiology and Biochemistry, National Taiwan University, Taipei, Taiwan 1061, [§]Department of Styling and Cosmetology, Hsin Sheng College of Medical Care and Management, Taoyuan, Taiwan 325, and [#]Department of Beauty Science, Meiho Institute of Technology, Pingtung, Taiwan 912. [‖] These two authors contributed equally.

Heavy metals are toxic to most living organisms and cause health problems by contaminating agricultural products. In plants, phytochelatin synthase (PCS, EC 2.3.2.15) uses glutathione (GSH) as its substrate to catalyze the synthesis of heavy metal-binding peptides, known as phytochelatins (PC). PCS has been described as a constitutive enzyme that may be controlled by post-translational modifications. However, the detailed mechanism of its catalytic activity is not clear. In this study, in vitro experiments demonstrate that PCS activity increased following phosphorylation by casein kinase 2 (CK2) and decreased following treatment with alkaline phosphatase. Site-directed mutagenesis experiments at amino acids on AtPCS1 indicate that Thr 49 is the site for phosphorylation. This is further supported by fact that the mutant AtPCS1(T49A) cannot be phosphorylated, and its activity is significantly lower than that of the wild-type enzyme. In the modeled three-dimensional structure of AtPCS1, Arg 183 is within close proximity to Thr 49. The mutant AtPCS1-(R183A) can be phosphorylated, but it shows much lower catalytic activity than the wild-type protein. This result suggested that Arg 183 may play an important role in the catalytic mechanism of AtPCS1. The possibility of the presence of a second substrate-binding site as a result of the interaction of these two amino acids is discussed. In addition, the activity of AtPCS1 was also found to be modulated by the C-terminal domain. The N-terminal catalytic domain of AtPCS1 was expressed (AtPCS1-N), and its catalytic activity was found to be even more sensitive to Cd or phosphorylation status than was the full-length enzyme.

KEYWORDS: Phytochelatin; phytochelatin synthase; protein phosphorylation; enzyme regulation

INTRODUCTION

Phytochelatins (PC) are short peptides synthesized from glutathione (GSH, γECG). They were found primarily in plants or fission yeast, where they function in the sequestration of invading heavy metals (*1*, *2*). In the cell, the biosynthesis of PCs is catalyzed by the enzyme phytochelatin synthase (PCS, EC 2.3.2.15) (*3*), which is a γ-glutamyl-cysteine transpeptidase with a papain-like catalytic triad (*4*−*7*). PCS produces its shortest product (PC_2) by linking together two molecules of GSH. The active Cys moiety on the catalytic triad attacks the carbonyl carbon of the Cys−Gly peptide bond on the first GSH. The Gly is then released, and part of the γEC links to the enzyme through acylation. The α-amino group on the N-terminal Glu of the second GSH then attacks the same carbonyl carbon on the γEC of acyl-enzyme and produces γECγECG (PC_2) as the product (*4*, *8*).

Arabidopsis PCS (AtPCS1) contains 485 amino acids and consists of an N-terminal and a C-terminal domain (*9*, *10*). The N-terminal domain of AtPCS1 shows 45% sequence identity to PCS from fission yeast (*11*, *12*); this domain contains the catalytic triad (Cys 56, His 162, and Asp 180 in AtPCS1). The C-terminal domain of PCS molecules from different species shows low sequence conservation but shares a common feature in that they all contain multiple Cys residues, often in pairs, and they bind Cd with high affinity and high capacity (*9*). Therefore, the C-terminal domain has been proposed to serve as the "sensor" of environmental Cd concentrations (*13*−*15*). The multiple Cys residues may bind heavy metals and bring them into contact with the active site in the N-terminal domain of PCS (*4*, *16*).

It was found that AtPCS1 is constitutively expressed in the levels of transcription and translation (*13*, *17*), suggesting that the enzyme may be regulated at the post-translational level. A previous study showed that PCS activity is active only in the presence of heavy metal ions (*3*). PC is biosynthesized until it has chelated and removed the heavy metals in the environment. This provides a mechanism of autoregulation to balance the cellular Cd concentration and PCS activity (*18*). Furthermore, protein phosphorylation, which is an essential post-translational modification in the cell, may alter the conformation of

*Address correspondence to this author at AC2-520, Department of Biochemical Science and Technology, National Taiwan University, Taipei, Taiwan 10617 (telephone 886-2-3366-4448; e-mail juang@ntu.edu.tw).

 Published on Web 08/04/2009

the protein and its catalytic activity. A large proportion of cellular proteins is regulated by protein phosphorylation. Possible phosphorylation sites on a protein can be predicted from the amino acid sequence using computer programs such as MyHits (*19*) and NetPhos (*20*). This led us to further investigate the phosphorylation of PCS and to determine how this modification affects the catalytic site and, concomitantly, enzymatic activity.

The prokaryotic counterpart of PCS from the cyanobacterium *Nostoc* sp. PCC 7120 (NsPCS) shows complete lack of the C-terminal domain of the eukaryotic enzymes (*21*, *22*). NsPCS is unique in that it catalyzes the deglycylation of GSH to γEC at a high rate and the synthesis of PC_2 at a relatively low rate (*23*). Recently, Vivares et al. (*5*) solved the crystal structures of NsPCS with its γEC acyl-enzyme intermediate. These studies confirm that PCS is closely related to the cysteine proteases, with a conserved catalytic triad in the active site (*7*). Moreover, the structure of the enzyme−GSH complex reveals a γEC acyl-enzyme intermediate lying in a cavity of the active site adjacent to a second putative GSH binding site. Because the amino acid sequence of NsPCS shows 36% identity with the N-terminal region of AtPCS1, the NsPCS crystal structure can serve as a template to model the N-terminal domain of AtPCS1. In addition to the full-length AtPCS1, we expressed a truncated version of the N-terminal domain of AtPCS1(AtPCS1-N). AtPCS1-N showed catalytic properties similar to those of full-length AtPCS1, but it also displayed unique behaviors that may be caused by the lack of the C-terminal region of the enzyme. In addition to identifying a phosphorylation site near the active site, we investigated the molecular details of the catalytic and regulatory mechanisms of PC synthesis.

MATERIALS AND METHODS

Recombinant Protein Expression of Full-Length and Truncated AtPCS1 Variants. *Arabidopsis* tissue (15-day seedling, 2 g) was harvested and ground in liquid nitrogen. Total RNA was isolated using TRIZOL reagent (Invitrogen) according to the manufacturer's instructions. The cDNA was synthesized from 5 μg of total RNA using the Superscript II RNase H reverse transcriptase (Invitrogen). The sequences encoding AtPCS1 (accession no. At5g44070), AtPCS-N (residues 1−221), and AtPCS-C (222−485) were amplified by the Polymerase Chain Reaction (PCR) using the following primer pairs: AtPCS1, 5′-GCTAGCGCGAGTTTATATCGGCGATC-3′ (AtPCS1 forward) and 5′-GGATCCCTAATAGGCAGGAGCAGCG-3′ (AtPCS1 reverse); AtPCS1-N, AtPCS1 forward primer and 5′-TTTGGATCCCTATCTGTGTGGTCTAGATATGAGC-3′ (AtPCS1-N reverse); AtPCS1-C, 5′-TTTGCTAGCGAACCCGGATTGCTCTATACTCTG-3′ (AtPCS1-C forward) and AtPCS1 reverse primer. The coding sequences were cloned into the pGEM-T-Easy vector (Promega) and sequenced.

The amplicons of the three AtPCS1 constructs were digested with *Nhe*I and *Bam*HI and subcloned into the pET28b vector (Novagen) as an in-frame fusion with a hexahistidine tag on the N-terminus. The identities of the three constructed plasmids were verified by DNA sequencing. The plasmids were then transformed into *Escherichia coli* BL21 (DE3) cells (Novagen) and selected on kanamycin plates. Protein expression was induced by 1 mM isopropyl β-D-1-thiogalactopyranoside (IPTG) for 4 h at 30 °C. The cultures of these transformants were then harvested, resuspended in ice-cold lysis buffer (25 mM Tris-HCl, pH 8.0, 1 mM DTT, 0.5 mM NaCl, 0.1% Tween 20, with protease inhibitor cocktail, Sigma P8849), and disrupted by the Cell Disruption System (Constant Systems, U.K.). The lysate was centrifuged for 30 min at 15000 rpm (Beckman Avanti J25, rotor JA 25.5) and filtered through a 0.45 μm syringe filter (Millipore). The supernatant was loaded onto a HisTrap FF column (GE Healthcare) preequilibrated with equilibration buffer (25 mM Tris-HCl, pH 8.0, 500 mM NaCl, 10% glycerol). After a washing with buffer containing 50 mM imidazole, the recombinant proteins were eluted with 200 mM imidazole. The eluates were concentrated and desalted by Amicon Ultra (cutoff size of 5000) (Millipore). The concentrations of the purified proteins were estimated according to the dye-binding Bradford method (*24*) using the microassay system from Bio-Rad (Protein Assay Kit). Bovine serum albumin was used as the protein standard.

Site-Directed Mutagenesis of Truncated AtPCS1 Variants. To investigate the roles of Thr 49, Tyr 55, and Arg 183, a single mutation was introduced into AtPCS1 or AtPCS1-N using the QuikChange Site-Directed Mutagenesis kit (Stratagene). Six mutants were derived from AtPCS1 or AtPCS1-N: AtPCS1(T49A), AtPCS1(Y55A), AtPCS1-(R183A), AtPCS1-N(T49A), AtPCS1-N(Y55A), and AtPCS1-N-(R183A). The primer 5′-GTTGATTTCGTATTTTCAG**GCG**CAATCCGAACCTGCGTATTG-3′ and its complementary oligonucleotides were used to change Thr 49 to Ala 49. The primer 5′-CACAATCCGAACCTGCG**GCG**TGTGGTTTGGCTAGTC-3′ and its complementary oligonucleotides were used to change Tyr 55 to Ala 55. The primer 5′-GAGATATGGCTTTGATTCTTGATGTTGCT**GCG**TTCAAGTATCC-3′ and its complementary oligonucleotides were used to change Arg 183 to Ala 183. The recombinant proteins were produced and purified as described above.

SDS-PAGE and Western Blot Analysis. SDS-PAGE was performed according to the method described by Laemmli (*25*), with a slight modification, using the mini-slab gel system (Amersham SE250). After electrophoresis, proteins were either stained with Coomassie Brilliant Blue R-250 or transferred to PVDF membranes (Immobilon-P, Millipore) in a Mighty Small Transphor (Amersham TE22) at 0.4 A for 2 h in transfer buffer (10 mM CAPS containing 10% methanol, pH 11). The protein blot was washed overnight with 6 M urea in phosphate-buffered saline containing 0.05% Tween 20 (PBST) to remove SDS and partially renature the protein for immunostaining. The blot was then washed three times with PBST. The washed blot was immersed in a solution of primary antibody diluted in gelatin−NET (0.25% gelatin, 0.15 M NaCl, 5 mM EDTA, 0.05% Tween 20 in 50 mM Tris-HCl, pH 8.0) and incubated at 4 °C for 3 h. The blot was then washed three times with PBST. The horseradish peroxidase-conjugated secondary antibody (goat anti-mouse IgG) diluted in gelatin−NET (1:5000) was then added. After incubation at room temperature for 2 h, the blot was washed three times with PBST. The bands were stained by adding the substrate solution of enhanced chemiluminescence reagent (VisGlow Plus Chemiluminescent Substrate, Visual Protein) to reveal the target proteins and analyzed by the AutoChemi System (UVP, U.K.). The monoclonal antibodies against the phosphoamino acids were obtained from Millipore (anti-phosphotyrosine clone 4G10 Platinum, 05-1050) or Sigma (anti-phosphothreonine clone PTR-8, P3555, and anti-phosphoserine clone PSR-45, P3430).

Assays for PCS Activity. The standard phytochelatin synthase activity assay was performed at 37 °C for 30 min in 100 μL reaction mixtures containing 50 mM Tris-HCl (pH 7.6), 1 mM DTT, 10% (w/v) glycerol, 10 mM GSH, 0.1 mM $CdCl_2$, and 8 μg of AtPCS1. In the case of the two truncated constructs, AtPCS1-N and AtPCS1-C, 4 μg was used instead. Prior to RP-HPLC analysis, the reaction mixture was acidified by adding 10 μL of 5% (v/v) trifluoroacetic acid and centrifuged at 14000 rpm for 30 min. Aliquots (25 μL) from individual reaction mixtures were analyzed by HPLC using a reverse-phase column (LiChrospher 100 RP-18e, Merck). A linear concentration gradient (0−20%) of acetonitrile, containing 0.05% trifluoroacetic acid, was used for the elution of phytochelatins, which were measured and converted into moles of GSH by comparison with the standard GSH peak. PCS activity was defined as the GSH mole equivalent of PC_2 and PC_3 produced per mole of enzyme per minute. Because only PC_2 and PC_3 were calculated for the product of the reaction, the enzyme activity observed in this study might be smaller than that found in other studies.

Assays for the Protein Phosphorylation by Casein Kinase 2. Phosphorylation by casein kinase 2 (CK2, New England BioLabs, P6010) was assayed by measuring the transfer of ^{32}P from [γ-^{32}P]ATP to the protein substrate (expressed AtPCS1 or variants). The reaction mixture contained 20 mM Tris-HCl (pH 7.5), 10 mM $MgCl_2$, 50 mM KCl, 3.7×10^4 Bq [γ-^{32}P]ATP, and 6 μg of target protein as the substrate. This mixture was incubated at 30 °C for 2 h, terminated by the addition of SDS sample buffer (*25*), and denatured at 100 °C for 10 min. After gel electrophoresis (13% SDS-PAGE) at 150 V, the gel was exposed on an imaging plate and visualized by an image analyzer (Fujix BAS 1000). To quantitate the radioactivity of the phosphorylated proteins, bands were

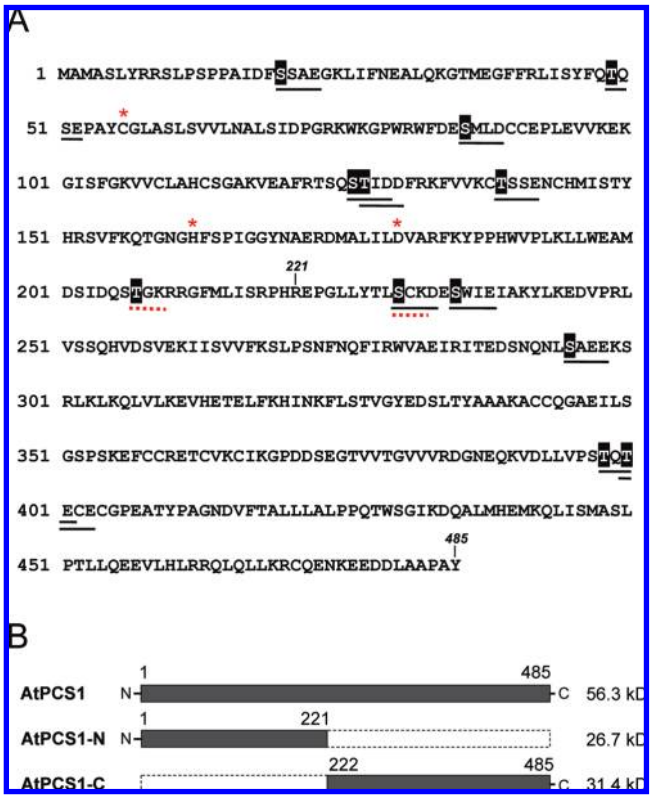

Figure 1. AtPCS1 sequence and the prediction of phosphorylation motifs. (**A**) The AtPCS1 sequence contains several phosphorylation sites that may be recognized by casein kinase 2 (CK2 sites underlined, [ST]-$X_{(2)}$-[DE]) or protein kinase C (PKC sites marked with dotted lines, [ST]-X-[RK]), as predicted by the programs MyHits and NetPhos. Residues in the proposed cysteine−protease catalytic triad are marked with asterisks. (**B**) Schematic diagram for the truncated AtPCS1 constructs AtPCS1-N and AtPCS1-C. Numbering on the bar diagram refers to the untagged sequence of the original AtPCS1 (485 amino acids). AtPCS1-N contains the first N-terminal 221 amino acids (1−221) and AtPCS1-C the remaining 264 amino acids of the C-terminal domain (222−485). The estimated molecular masses of the expressed proteins are listed to the right of each construct.

cut out directly from the gel after staining and placed in counting vials. After addition of the scintillation fluid, the radioactivity was measured in a liquid scintillation counter (Beckman LS 5000).

PCS Molecular Modeling. The structure of phytochelatin synthase from the cyanobacterium *Nostoc* has been determined using X-ray crystallography (PDB code 2BU3) (*5*). The N-terminal domain (residues 12−218) of *Arabidopsis* PCS shows 33% sequence identity and 51% sequence similarity to the corresponding part of *Nostoc* phytochelatin synthase. The molecular model of AtPCS1 (residues 12−218) was generated using the coordinates of 2BU3 as template by Discovery Studio 2.0 software (Accelrys). The model was subjected to energy minimization and validated using Protein Health within Discovery Studio. The substrate γ-glutamylcysteine was transferred into the model from the template crystal structure.

RESULTS AND DISCUSSION

Phytochelatin Synthase Expressed in *E. coli* Is Phosphorylated at a Thr Residue Near Its Catalytic Site on the N-Terminal Domain. From the amino acid sequence of *Arabidopsis* PCS, several sites were predicted to be potential phosphorylation motifs that could be phosphorylated by casein kinase 2 (CK2) or protein kinase C (**Figure 1A**). Indeed, using specific monoclonal antibodies against phospho-amino acids, we found that full-length PCS (AtPCS1) expressed in *E. coli* was phosphorylated on its Tyr or Thr residues (**Figure 2A**). Two truncated fragments of AtPCS1 were constructed and expressed in *E. coli* (AtPCS1-N and AtPCS1-C, **Figure 1B**). The AtPCS1-N fragment contained the N-terminal domain of PCS, and the AtPCS1-C contained the C-terminal domain of the protein. Only AtPCS1-N was phosphorylated on its Tyr or Thr residues. Neither of the fragments was phosphorylated on Ser residues (**Figure 2A**). The expressed full-length AtPCS1 and two domains were then phosphorylated in vitro by CK2 in the presence of radioactive ATP. The autoradiograph showed that both AtPCS1 and AtPCS1-N were phosphorylated by CK2, whereas phosphorylation of AtPCS1-C was not detected (**Figure 2C**). The radioactive phosphate group on phosphorylated AtPCS1 could be removed by calf intestine alkaline phosphatase (CIAP; **Figure 2D**).

CK2 contains two identical catalytic subunits (α, 44 kDa) and two identical regulatory subunits (β, 26 kDa). These subunits were allowed to undergo autophosphorylation, giving rise to two bands on the autoradiograph. Because the molecular masses of AtPCS1-N and the CK2 β subunit are very similar, it was difficult to resolve these two bands on the gel. However, by comparing the relative intensity of the bands on the autoradiograph, and the Coomassie Brilliant Blue stained bands of AtPCS1-N, we concluded that the AtPCS1-N fragment was phosphorylated. This conclusion was further confirmed in experiments using only the catalytic α subunit of CK2 to phosphorylate AtPCS1 (**Figure 3B**) and AtPCS-N (**Figure 3C**). In these experiments, the β subunit was not present to interfere with the interpretation of the results.

The phosphorylation of AtPCS1 by CK2 depended on the concentration of Cd; at least 30 μM Cd was needed to trigger the phosphorylation (**Figure 3A**). Interestingly, this reaction was blocked by the substrate GSH (**Figure 3B**). However, the oxidized form of GSH (GSSG) did not show such an inhibitory effect (lane 9 in **Figure 3B**). To our surprise, AtPCS1-N was phosphorylated independent of the concentration of Cd or the presence of GSH (**Figure 3C**). It is possible that GSH makes Cd unavailable to PCS in the reaction mixture, because GSH has a higher binding affinity for Cd. If the cellular GSH decreases or the invading Cd increases, the Cd may become available and induce the phosphorylation of PCS. One possible model for the above observations is that Cd binds to the C-terminal domain and triggers a conformational change that exposes the phosphorylation site on the N-terminal domain. This model would explain why the prokaryotic enzymes are not sensitive to heavy metals (*21*, *22*), because the prokaryotic PCS lacks a C-terminal domain. Taking away the C-terminal domain removes the Cd dependence of the phosphorylation and leads to constitutive phosphorylation, as observed with AtPCS1-N (**Figure 3C**). Three-dimensional structural information of AtPCS1 would help to elucidate the mechanism.

The Activity of PCS Requires Cd and Is Enhanced by Protein Phosphorylation. Cd is critical to the catalytic activities of both AtPCS1 and AtPCS1-N, but to different extents (**Figure 4A**). If Cd was not added in the reaction mixture, AtPCS1 activity decreased to 50% of its full activity. However, in the absence of Cd, AtPCS1-N activity was $<20\%$ of its full activity. The activities of both AtPCS1 and AtPCS1-N decreased if they were dephosphorylated by CIAP (lane 2 in **Figure 4B**). However, the lost activity could be fully recovered by subsequent phosphorylation with CK2 (lane 3). The N-terminal domain (AtPCS1-N) was more sensitive than the full-length PCS to Cd concentration and phosphorylation (**Figure 4**). Moreover, the mutants of AtPCS1 or AtPCS1-N demonstrated a similar tendency. AtPCS1-N mutants showed only slight activity (**Figure 5D**), but AtPCS1 mutants retained partial activity in the presence of Cd (**Figure 5C**). These observations imply that the C-terminal half may play a role in

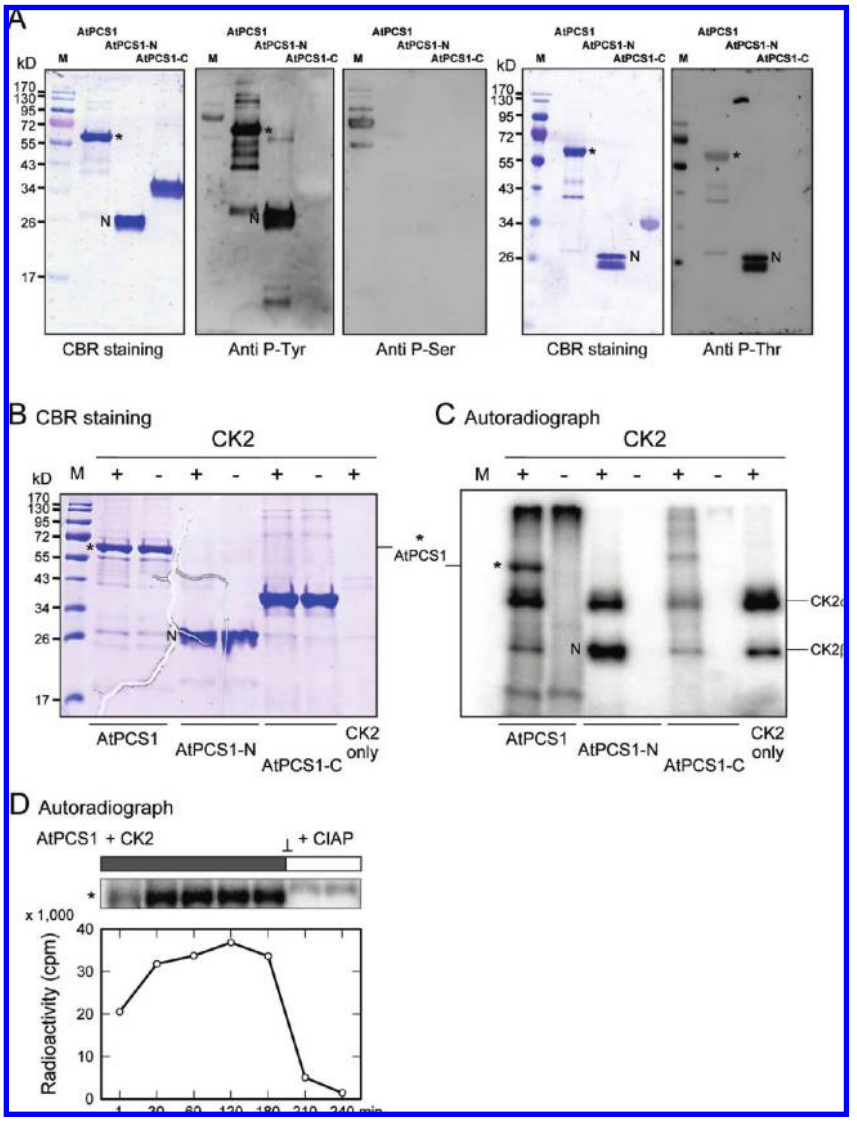

Figure 2. PCS expressed from *E. coli* is phosphorylated, and the phosphorylation can be catalyzed in vitro by casein kinase 2. (**A**) Expressed AtPCS1, AtPCS1-N, and AtPCS1-C were purified and separated by SDS-PAGE (6 μg of protein per lane), and then the phosphorylated proteins were detected by monoclonal antibodies against phospho-Tyr (P-Tyr), phospho-Ser (P-Ser), and phospho-Thr (P-Thr). Full-length AtPCS1 bands are marked with asterisks, and the AtPCS1-N fragments are indicated with the letter "N". (**B**, **C**) CK2 phosphorylated AtPCS1 and AtPCS1-N, but not AtPCS1-C. (**D**) The phosphorylation of PCS was reversed by the addition of calf intestine alkaline phosphatase (CIAP), after the phosphorylation reaction had been terminated using the CK2 inhibitor heparin (marked with an inverted "T"). The radioactive bands of the phosphorylated PCS were also measured by liquid scintillation counting to measure the level of phosphorylation.

regulating the activity of PCS and maintain a basal level of activity.

It is arguable that in the absence of Cd we can constantly measure 50% of the full catalytic activity for the full-length AtPCS1 (**Figures 4A** and **5C**), because previous study showed that PCS activity is active only in the presence of heavy metal ions (*3*). One possibility is that our enzyme preparation might be contaminated by a trace amount of Ni during the elution of the expressed protein from HisTrap FF column. However, this observation might be not simply an artifact of contamination; it could be the consequence of the phosphorylation to the enzyme, which helps in forming a competent active site for accommodating the substrates. In **Figure 5C**, the mutant T49A of AtPCS1 cannot be phosphorylated, and it lost all its catalytic activity in the absence of Cd. This observation indicates that both Cd and phosphorylation were involved in the catalysis of PCS. Furthermore, Vatamaniuk et al. (*17*) reported that free metal ions are not essential for the activity of AtPCS1, because the enzyme can catalyze the synthesis of *S*-alkyl PC_n from *S*-alkyl GSH derivatives in the absence of heavy metals. Their observation indicates that heavy metal ions do not activate catalysis through direct interaction with the enzyme but instead do so through interaction with the substrate.

Thr 49 and Arg 183 Are Critical to the Catalytic Activity of PCS; However, Thr 49 Is the Only Residue To Be Phosphorylated. From the amino acid sequence of PCS, Thr 49 and its neighboring amino acids on the C-terminal side (TQSE) were predicted to be a strong phosphorylation signal for CK2 (**Figure 1A**). Indeed, site-directed mutagenesis of amino acids near the catalytic area showed Thr 49 to be the principal phosphorylation site on AtPCS1 (**Figure 5A**,**B**). Autoradiography demonstrated that the mutant AtPCS1(T49A) was phosphorylated very slightly, whereupon its catalytic activity decreased to 50% that of the wild-type enzyme (**Figure 5C**). The activity of the N-terminal mutant AtPCS1-N(T49A) declined even

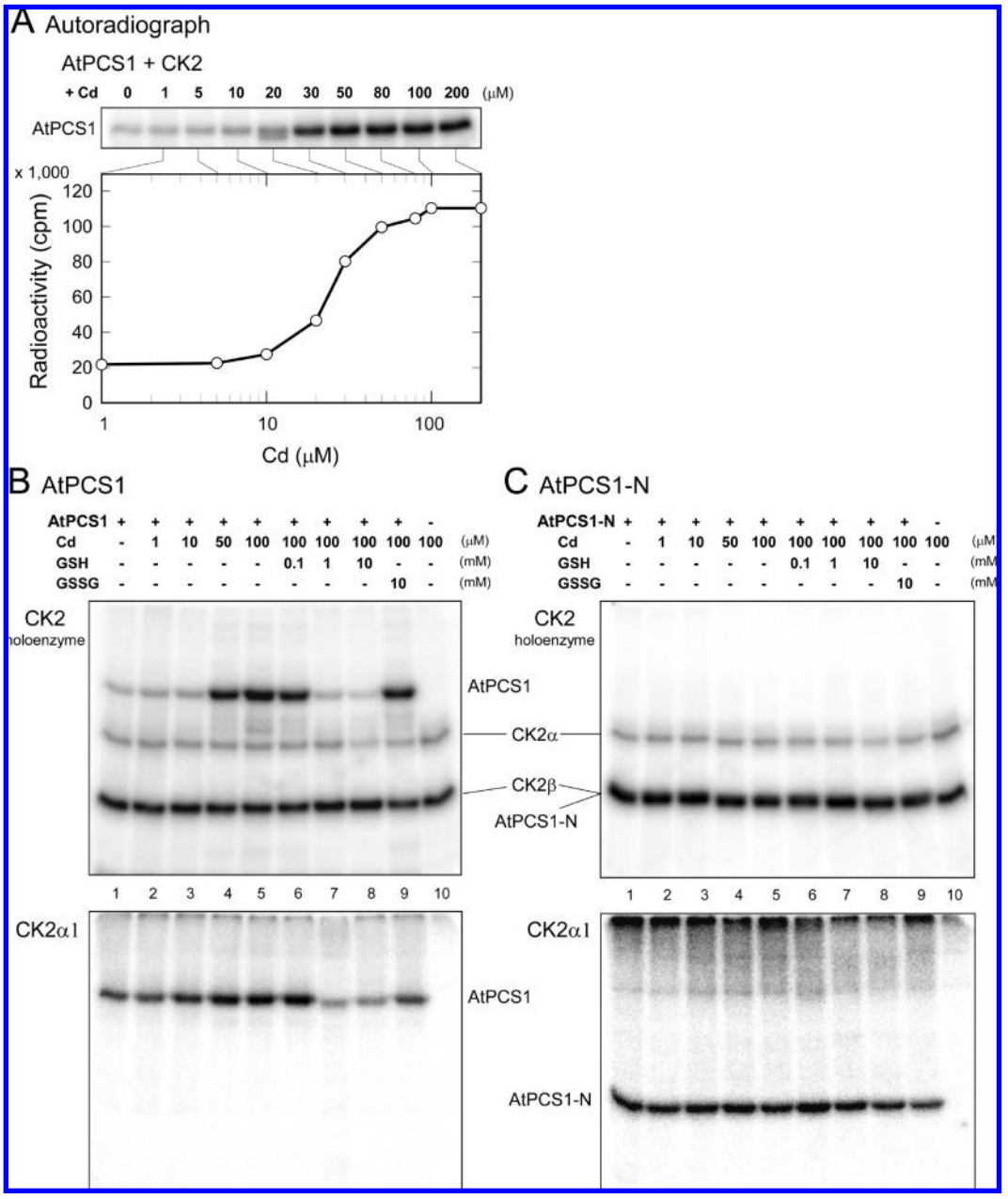

Figure 3. The phosphorylation of AtPCS1 is Cd-dependent and is blocked by glutathione. (**A**) The phosphorylation of AtPCS1 by CK2 depended on the concentration of Cd. Cd at a concentration of at least 30 μM was required to trigger the phosphorylation under our experimental conditions. (**B**) The phosphorylation of the full-length AtPCS1 was blocked by its substrate, GSH. Interestingly, the oxidized form of glutathione (GSSG) had no such inhibitory effect. (**C**) The phosphorylation of AtPCS1-N was independent of Cd, and it was not affected by GSH. Because autophosphorylation of the CK2 β subunit interfered with the observation of the phosphorylated AtPCS1-N (upper autoradiograph in **C**), we used the expressed α1 catalytic subunit (CK2α1) to visualize the AtPCS1-N band (lower autoradiograph in **C**).

more extensively, to $<20\%$ of wild-type activity (**Figure 5D**). Arg 183 is one of the consensus amino acids located near the catalytic site. The mutant R183A was phosphorylated, which reduced its activity even more than that of the T49A mutants (**Figure 5C**,**D**). In all cases, Cd was critical for PCS activity (open bars in **Figure 5C**,**D**), although AtPCS1-N showed a stronger dependence on Cd.

The three-dimensional structure of NsPCS (*5*) was used as the template for the computer-aided modeling of the N-terminal domain of PCS. **Figure 6** shows the active site of PCS, including the catalytic triad, γEC, Arg 183, and the phosphorylation site (P-Thr 49). The inset at the upper right corner of **Figure 6** is a schematic diagram of the critical features around this catalytic area where important amino acids are arranged along two segments of the protein. The lower frame (dark blue) contains a segment of coil extending from Phe 47 to Cys 56. The upper frame (dark purple) also shows a coil, from Asp 180 to Pro 188. These two coils may interact through the side chain of Arg 183 and the phosphate group of the phosphorylated Thr 49. This interaction may serve as a "molecular clip" to give the active site a conformation appropriate for catalysis. In particular, the interaction may bring together the residues of the catalytic triad (inset in **Figure 6**). Furthermore, the interaction between phospho-Thr 49 and Arg 183 may create a cavity in the active site (marked with asterisks in **Figure 6**) that may serve as the second binding site for the next GSH to react with the γEC of the acyl-enzyme.

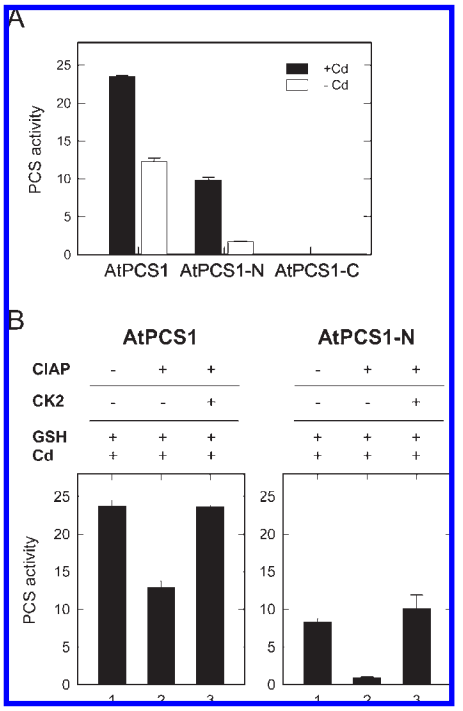

Figure 4. The activity of PCS depends on Cd and is activated by phosphorylation. (**A**) Cd enhanced the catalytic activity of both AtPCS1 and AtPCS1-N. In particular, AtPCS1-N lost nearly all of its activity in the absence of Cd. The C-terminal AtPCS1-C showed no activity under any conditions tested. (**B**) Treating AtPCS1 and AtPCS1-N with alkaline phosphatase (CIAP, lane 2) reduced their activity, but this could be restored by phosphorylation with CK2 (lane 3). All activity assays were carried out using an equimolar ratio of proteins (8 μg of AtPCS1 and 4 μg of AtPCS1-N) and 30 mM GSH. The horizontal lines in (**B**) represent 30 min of incubation at 37 °C. Vertical bars represent the standard error of the mean (n = 3).

Alignment and comparison of the amino acid sequences of PCS from several species, including the cyanobacterium *Nostoc*, showed that Thr 49 is conserved (*5*). However, the Thr residue in *Nostoc* is followed by QVN, and TQVN is not a competent phosphorylation target for CK2. Therefore, phosphorylation was not predicted at this residue for the *Nostoc* enzyme. If that were the case, the lack of protein phosphorylation may make the second GSH-binding site difficult to form in NsPCS, and that may explain why this prokaryotic enzyme is not as efficient as the eukaryotic enzymes at synthesizing PCs (*21*, *22*).

PCS is a constitutively expressed, ubiquitous enzyme in *Arabidopsis* (*17*). It is therefore important to understand the post-translational modification or regulation of PCS, because this likely affects its activity in the cell. Cd was the first factor found to increase PCS activity, and the metal may interact with GSH to form the Cd−GS_2 complex, or it may bind directly to the enzyme. Although the C-terminal domain is thought to bind Cd (*13*), it is possible that Cd binds directly to the catalytic site. On the other hand, our study showed that phosphorylation status may also affect PCS activity. Besides, the phosphorylation of PCS is Cd-dependent and is inhibited by the presence of GSH. Apparently, Cd, GSH, and phosphorylation might work together and produce a regulation pathway for PCS activity. More interestingly, the amino acid phosphorylated could interact with its neighboring Arg residue to shape up a competent active conformation for the second substrate, which suggested a possible mechanism for the elongation of PC molecule. We are now exploring the cellular effect of the phosphorylation on AtPCS1 to the heavy metal tolerance of *Arabidopsis*. If the phosphorylation was also observed in vivo, then a protein kinase for PCS, and probably a route of signal transduction leading to the activation of this kinase, may be identified in the cell.

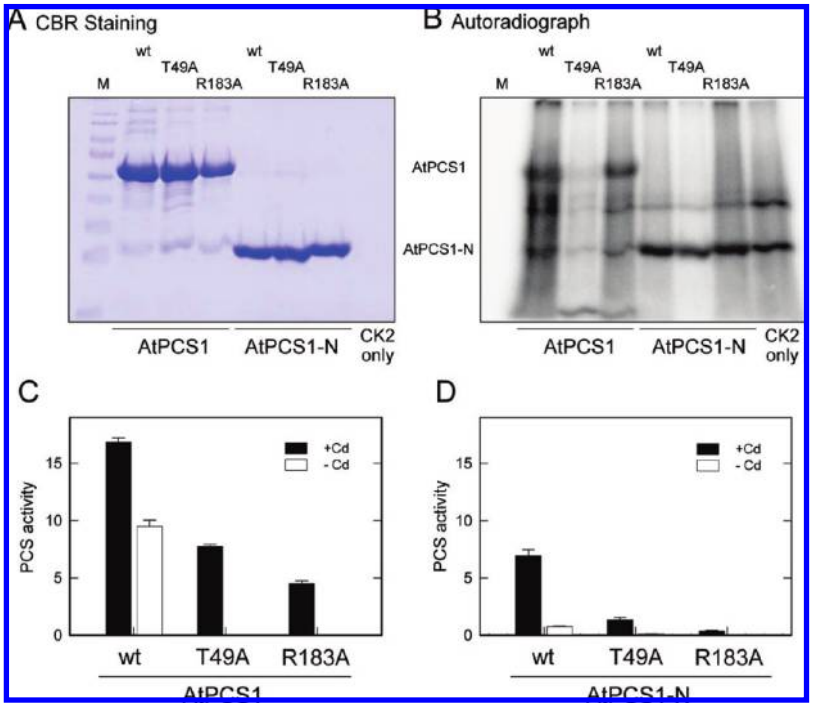

Figure 5. AtPCS1 is phosphorylated at Thr 49 by CK2, and both Thr 49 and Arg 183 are critical to the activity of PCS. (**A**, **B**) Site-directed mutagenesis of AtPCS1 and AtPCS1-N at Thr 49 (T49A) or Arg 183 (R183A) showed that phosphorylation of PCS occurs at Thr 49. (**C**, **D**) The catalytic activity was lower than that of the wild type for all mutants (T49A and R183A) derived from AtPCS1 (**C**) or AtPCS1-N (**D**). Vertical bars represent the standard error of the mean (n = 2).

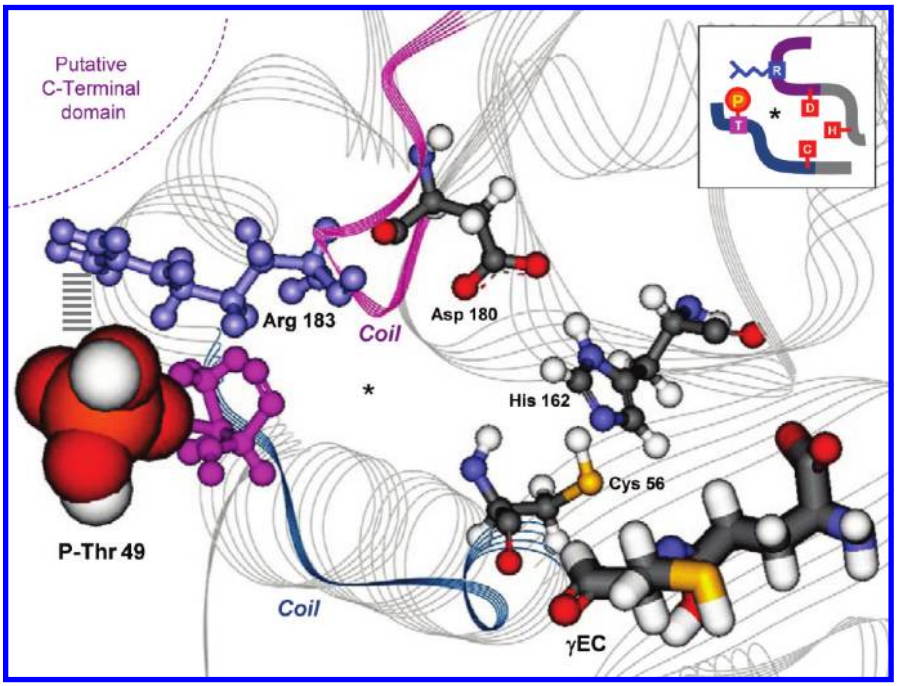

Figure 6. Phosphorylation may play an important role in helping the active site of PCS achieve a functional conformation. The molecular model for the N-terminal domain of PCS (AtPCS1-N) was generated with Discovery Studio (Accelrys) software using the crystal structure of NsPCS as the template (*5*). The C-terminal domain was not included, because NsPCS has only the N-terminal half of AtPCS1. The catalytic site of AtPCS1 is occupied by a γEC, and the postulated second substrate binding sites are marked with asterisks. It is important to note that the modeling places the side chain of Arg 183 very close to the phosphate group of phospho-Thr 49. A schematic diagram (inset at upper right corner) illustrates the fact that these critical amino acids are located on two coils around the catalytic site. Interaction between the phosphorylated Thr 49 and the Arg 183 may bring these two coils together to achieve a functional conformation for the catalytic site of PCS.

ABBREVIATIONS USED

CIAP, calf intestine alkaline phosphatase; CK2, casein kinase 2; GSH, glutathione; PC, phytochelatin; PCS, phytochelatin synthase.

ACKNOWLEDGMENT

We thank Dr. David Ow (PGEC, ARS, USDA, Albany, CA) for reading the manuscript and helpful suggestions. We are also grateful for the excellent technical assistance from the Technology Commons (TechComm), College of Life Science, National Taiwan University.

LITERATURE CITED

(1) Grill, E.; Winnacker, E. L.; Zenk, M. H. Phytochelatins: the principal heavy-metal complexing peptides of higher plants. *Science* **1985**, *230*, 674–676.

(2) Murasugi, A.; Wada, C.; Hayashi, Y. Purification and unique properties in UV and CD spectra of Cd-binding peptide 1 from *Schizosaccharomyces pombe*. *Biochem. Biophys. Res. Commun.* **1981**, *103*, 1021–1028.

(3) Grill, E.; Loffler, S.; Winnacker, E. L.; Zenk, M. H. Phytochelatins, the heavy-metal-binding peptides of plants, are synthesized from glutathione by a specific γ-glutamylcysteine dipeptidyl transpeptidase (phytochelatin synthase). *Proc. Natl. Acad. Sci. U.S.A.* **1989**, *86*, 6838–6842.

(4) Rea, P. A.; Vatamaniuk, O. K.; Rigden, D. J. Weeds, worms, and more. Papain's long-lost cousin, phytochelatin synthase. *Plant Physiol.* **2004**, *136*, 2463–2474.

(5) Vivares, D.; Arnoux, P.; Pignol, D. A papain-like enzyme at work: native and acyl-enzyme intermediate structures in phytochelatin synthesis. *Proc. Natl. Acad. Sci. U.S.A.* **2005**, *102*, 18848–18853.

(6) Romanyuk, N. D.; Rigden, D. J.; Vatamaniuk, O. K.; Lang, A.; Cahoon, R. E.; Jez, J. M.; Rea, P. A. Mutagenic definition of a papain-like catalytic triad, sufficiency of the N-terminal domain for single-site core catalytic enzyme acylation, and C-terminal domain for augmentative metal activation of a eukaryotic phytochelatin synthase. *Plant Physiol.* **2006**, *141*, 858–869.

(7) Rea, P. A. Phytochelatin synthase, papain's cousin, in stereo. *Proc. Natl. Acad. Sci. U.S.A.* **2006**, *103*, 507–508.

(8) Vatamaniuk, O. K.; Mari, S.; Lang, A.; Chalasani, S.; Demkiv, L. O.; Rea, P. A. Phytochelatin synthase, a dipeptidyltransferase that undergoes multisite acylation with γ-glutamylcysteine during catalysis: stoichiometric and site-directed mutagenic analysis of *Arabidopsis thaliana* PCS1-catalyzed phytochelatin synthesis. *J. Biol. Chem.* **2004**, *279*, 22449–22460.

(9) Vatamaniuk, O. K.; Mari, S.; Lu, Y. P.; Rea, P. A. AtPCS1, a phytochelatin synthase from *Arabidopsis*: isolation and *in vitro* reconstitution. *Proc. Natl. Acad. Sci. U.S.A.* **1999**, *96*, 7110–7115.

(10) Ruotolo, R.; Peracchi, A.; Bolchi, A.; Infusini, G.; Amoresano, A.; Ottonello, S. Domain organization of phytochelatin synthase—functional properties of truncated enzyme species identified by limited proteolysis. *J. Biol. Chem.* **2004**, *279*, 14686–14693.

(11) Clemens, S.; Kim, E. J.; Neumann, D.; Schroeder, J. I. Tolerance to toxic metals by a gene family of phytochelatin synthases from plants and yeast. *EMBO J.* **1999**, *18*, 3325–3333.

(12) Ha, S. B.; Smith, A. P.; Howden, R.; Dietrich, W. M.; Bugg, S.; O′Connell, M. J.; Goldsbrough, P. B.; Cobbett, C. S. Phytochelatin synthase genes from *Arabidopsis* and the yeast *Schizosaccharomyces pombe*. *Plant Cell* **1999**, *11*, 1153–1164.

(13) Cobbett, C. S. Phytochelatins and their roles in heavy metal detoxification. *Plant Physiol.* **2000**, *123*, 825–832.

(14) Ramos, J.; Clemente, M. R.; Naya, L.; Loscos, J.; Perez-Rontome, C.; Sato, S.; Tabata, S.; Becana, M. Phytochelatin synthases of the model legume *Lotus japonicus*. A small multigene family with differential response to cadmium and alternatively spliced variants. *Plant Physiol.* **2007**, *143*, 1110–1118.

(15) Ramos, J.; Naya, L.; Gay, M.; Abian, J.; Becana, M. Functional characterization of an unusual phytochelatin synthase, LjPCS3, of *Lotus japonicus*. *Plant Physiol.* **2008**, *148*, 536–545.

(16) Vestergaard, M.; Matsumoto, S.; Nishikori, S.; Shiraki, K.; Hirata, K.; Takagi, M. Chelation of cadmium ions by phytochelatin synthase: role of the cystein-rich C-terminal. *Anal. Sci.* **2008**, *24*, 277–281.

(17) Vatamaniuk, O. K.; Mari, S.; Lu, Y. P.; Rea, P. A. Mechanism of heavy metal ion activation of phytochelatin (PC) synthase: blocked thiols are sufficient for PC synthase-catalyzed transpeptidation of glutathione and related thiol peptides. *J. Biol. Chem.* **2000**, *275*, 31451–31459.

(18) Loffler, S.; Hochberger, A.; Grill, E.; Winnacker, E. L.; Zenk, M. H. Termination of the phytochelatin synthase reaction through sequestration of heavy metals by the reaction product. *FEBS Lett.* **1989**, *258*, 42–46.

(19) Pagni, M.; Ioannidis, V.; Cerutti, L.; Zahn-Zabal, M.; Jongeneel, C. V.; Hau, J.; Martin, O.; Kuznetsov, D.; Falquet, L. MyHits: improvements to an interactive resource for analyzing protein sequences. *Nucleic Acids Res.* **2007**, *35* (Web Server issue), W433−W437.

(20) Blom, N.; Gammeltoft, S.; Brunak, S. Sequence and structure-based prediction of eukaryotic protein phosphorylation sites. *J. Mol. Biol.* **1999**, *294*, 1351–1362.

(21) Tsuji, N.; Nishikori, S.; Iwabe, O.; Shiraki, K.; Miyasaka, H.; Takagi, M.; Hirata, K.; Miyamoto, K. Characterization of phytochelatin synthase-like protein encoded by alr0975 from a prokaryote, *Nostoc* sp. PCC 7120. *Biochem. Biophys. Res. Commun.* **2004**, *315*, 751–755.

(22) Harada, E.; von Roepenack-Lahaye, E.; Clemens, S. A cyanobacterial protein with similarity to phytochelatin synthases catalyzes the conversion of glutathione to gamma-glutamylcysteine and lacks phytochelatin synthase activity. *Phytochemistry* **2004**, *65*, 3179–3185.

(23) Tsuji, N.; Nishikori, S.; Iwabe, O.; Matsumoto, S.; Shiraki, K.; Miyasaka, H.; Takagi, M.; Miyamoto, K.; Hirata, K. Comparative analysis of the two-step reaction catalyzed by prokaryotic and eukaryotic phytochelatin synthase by an ion-pair liquid chromatography assay. *Planta* **2005**, *222*, 181–191.

(24) Bradford, M. M. A rapid and sensitive method for the quantitation of microgram quantities of protein utilizing the principle of protein−dye binding. *Anal. Biochem.* **1976**, *72*, 248–254.

(25) Laemmli, U. K. Cleavage of structural proteins during the assembly of the head bacteriophage T4. *Nature* **1970**, *227*, 680–685.

Received April 6, 2009. Revised manuscript received July 19, 2009. Accepted July 20, 2009.